Title

Ultrafast Charge-Transfer Dynamics in the Iron–Sulfur Complex of Rhodobacter capsulatus Ferredoxin VI

Journal

The Journal of Physical Chemistry Letters, 8(18)

ISSN

1948-7185

Authors

Mao, Ziliang
Carroll, Elizabeth C
Kim, Peter W
et al.

Publication Date

2017-09-21

DOI

10.1021/acs.jpclett.7b02026

Peer reviewed

HHS Public Access

Author manuscript

J Phys Chem Lett. Author manuscript; available in PMC 2020 April 28.

Published in final edited form as:

J Phys Chem Lett. 2017 September 21; 8(18): 4498–4503. doi:10.1021/acs.jpclett.7b02026.

Ultrafast Charge Transfer Dynamics in the Iron-Sulfur Complex of *Rhodobacter capsulatus* Ferredoxin VI

Ziliang Mao[†], **Elizabeth C. Carroll**[†,‡], **Peter W. Kim**[†,§], **Stephen P. Cramer**[*,†], **Delmar S. Larsen**[*,†]

[†]Department of Chemistry, University of California Davis, One Shields Avenue, Davis, California 95616, United States

Abstract

Iron-sulfur proteins play essential roles in various biological processes. Their electronic structure and vibrational dynamics are key to their rich chemistry, but nontrivial to unravel. Here the first ultrafast transient absorption and impulsive coherent vibrational spectroscopic (ICVS) studies on 2Fe-2S clusters in *Rhodobacter capsulatus* ferreodoxin VI are characterized. Photoexcitation initiated populations on multiple excited electronic states that evolve into each other in a long-lived charge transfer state. This suggests a potential light-induced electron-transfer pathway as well as the possibility of using iron-sulfur proteins as photosensitizers for light-dependent enzymes. A tyrosine chain near the active site suggests potential hole-transfer pathways and affirms this electron-transfer pathway. T0he ICVS data revealed vibrational bands at 417 cm^{-1} and 484 cm^{-1}, with the latter attributed to an excited-state mode. The temperature dependence of the ICVS modes suggests that temperature effect on protein structure or conformation heterogeneities needs to be considered during cryogenic temperature studies.

Graphical Abstarct

[*]**Corresponding Authors:** dlarsen@ucdavsi.edu & spjcramer@ucdavis.edu.

[‡]Department of Imaging Physics, Delft University of Technology, Postbus 5, 2600 AA Delft, The Netherlands

[§]Applied Biosciences and Engineering, Sandia National Laboratories, Livermore, CA 94550, USA

Supporting Information

The Supporting Information is available free of charge on the ACS Publications website. Experimental procedures, experimental setup diagrams, details about global analysis, and supporting results.

The authors declare no competing financial interests.

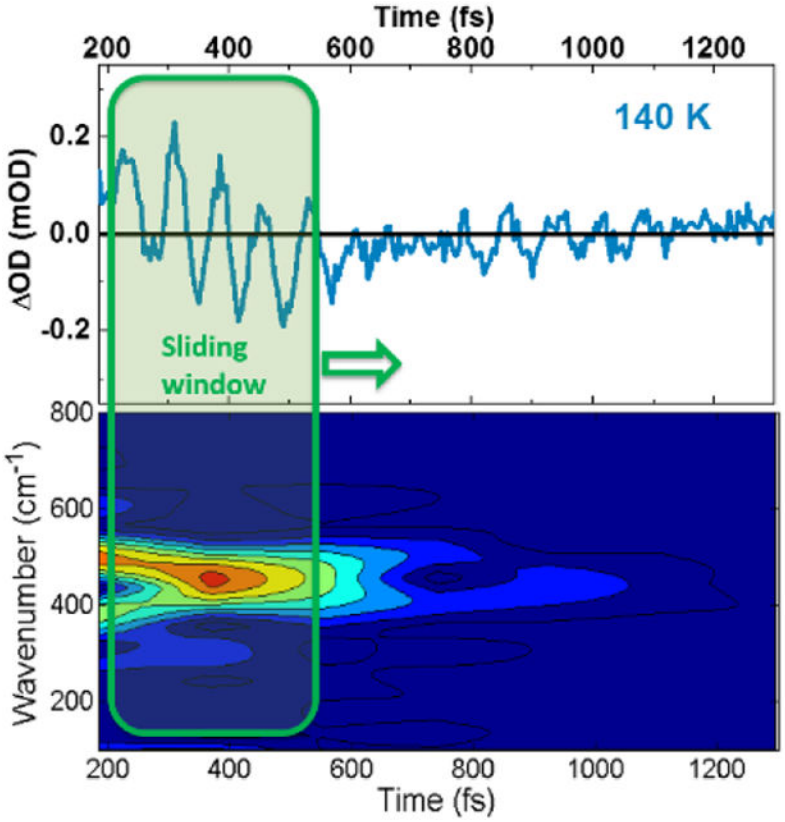

Keywords

Iron-sulfur cluster; ultrafast transient absorption; impulsive coherent vibrational spectroscopy; electron transfer; hole transfer; resonance Raman

Iron-sulfur (FeS) clusters are ubiquitous in nature and serve a wide range of functions, including electron transfer (ET), small-molecule sensing, and the catalysis of chemical reactions.[1] They also play key roles in various essential biological processes such as photosynthesis, cellular respiration and nitrogen fixation.[2] Since their discovery in the 1960s, FeS cluster proteins have been studied extensively, yet key questions about their structure-function paradigm remain. While it is clear that their electronic structure is essential for their rich chemistry, it is nontrivial to characterize due to its complexity and the fact a large number of states exist in close proximity.[3–4]

Recently, interest about photo-induced chemical processes involving FeS proteins has risen. For example, the involvement of FeS clusters in photosensitization in living cells[5] and photo-induced ET in the purple phototroph *Rhodoferax fermentans*[6] has been reported. The incorporation of external photosensitizers to hydrogenases and nitrogenases enabled photo-activated hydrogen production and nitrogen fixation.[7–9] Similarly, several Fe-Fe hydrogenase model compounds that contain FeS clusters were found to facilitate hydrogen production under sunlight without adding external photosensitizers.[10] This opens the

possibility of using FeS proteins and model compounds as photosensitizers for solar hydrogen production.

Of the many varied FeS clusters identified in nature, the 2Fe-2S clusters are the simplest multi-iron clusters for study. A representative protein that binds a 2Fe-2S cluster is the sixth ferredoxin (Rc6) discovered from *Rhodobacter capsulatus*,[11] which is involved in the synthesis of FeS clusters.[12] Its structure has been determined (Figure 1)[12] and resembles structures typical of 2Fe-2S ferredoxins that are critical ET proteins involved in a range of metabolic processes. Hence, Rc6 is an excellent model system for the time-resolved characterization of photo-induced dynamics in FeS clusters.

Here we report the first ultrafast transient absorption (TA) study on the electronic relaxation dynamics and impulsive coherent vibrational spectroscopic (ICVS) study on the vibrational relaxation dynamics of oxidized Rc6. We have used these techniques to obtain a better knowledge of the electronic and vibrational dynamics of the 2Fe-2S cluster. The TA technique probes the time-dependent change of sample absorbance upon laser excitation, and reveals information about excited-state population evolution, electron and proton transfer, and subsequent dynamics. The ICVS technique is a variant TA technique and has been used to study the vibrational dynamics of the mononuclear Fe site (1Fe-4S) in the *Pyrococcus furiosus* rubredoxin (*Pf*Rd) and the 7Fe-9S-1Mo cofactor (FeMoco) of the nitrogenase MoFe protein from *Azotobacter vinelandii*.[13–15] These studies identified key vibrational modes that are coupled to excited electronic states that participate in photo-induced electron-transfer processes.

To refine the models for the electronic and vibrational dynamics, cryogenic temperature (140 K) study was also performed to complement room temperature study. Lower temperature slows down the relaxation of excited-state dynamics as well as the dephasing of vibrational wave-packets and allows more refined characterization of the kinetics. Since most static spectroscopic studies on FeS proteins have been conducted at cryogenic temperatures, the 140 K study also establishes a point of comparison to previous studies.

The TA spectra of Rc6 at select delay times at both 292 K and 140 K are contrasted in Figure 2 (A) and (C)with corresponding kinetics at select wavelengths in Figure 2 (B) and (D). The kinetics are distinctly non-monotonic with dynamics extending over multiple time scales from fs to ns. The results are thus more complicated than the TA dynamics observed in the 1Fe-4S *Pf*Rd and 7Fe-9S-1Mo FeMoco in nitrogenase MoFe protein.[13, 15] At both temperatures, multiple contributions to the TA signals are observed: (1) A ground-state bleaching band at 460 nm, (2) A negative band at 480 nm, (3) A positive signal around 436 nm that appears immediately after excitation and persists for several ns, (4) A positive band around 565 nm at 292 K and 545 nm at 140 K. It appears earlier or stronger at 140 K where it grows in on several ps and then decays away after 6 ns. (5) A broad positive signal around 645 nm that is blue-shifted at 140 K relative to 292 K. It grows in within 100 fs and decays away after 1 ns.

Analysis of broadband TA signals was performed using a multi-component global analysis method.[16–17] A simple 4-compartment sequential model was adopted to fit the data to

estimate the underlying directly-observed timescales in the data (Figure 3). This model fits the TA signals well (Figure 2), suggesting that (at least) four populations are resolved in the data. Although the Evolution Associated Difference Spectra (EADS) extracted from this analysis are not the actual spectra of the constituent populations this anlysis serves as a useful measure to interpret the timescale and nature of the underlying dynamics (Figure 3B and 3C). Unfortunately, efforts to construct more "correct" models were unsuccessful and can be reviewed in the Supporting Information (Figure S6–S7).

As expected, the dynamics at 140 K are slower than the 292 K dynamics (Table S1).[18] The EADS of the sequential model (Figure 3B and 3C) share similar spectral characteristics with the raw TA spectra (Figure 2A and 2C). They all exhibit the ground-state bleach and stimulated-emission features at 460 nm and 480 nm, with excited-state absorption bands near 436 nm and in the long-wavelength region. The EADS3 and EADS4 are nearly identical below 600 nm, with two positive bands at 436 nm and 565 nm. These bands decay on the same timescale (Figure S5), and may represent either the same species or two species that are in equilibrium. We also notice that the 436 nm band is formed instantly and continues to grow within the first 2 ps, while a long-wavelength band near 625 nm forms instantly and decays away within 5 ps. This is suggestive that there may be multiple excited-state populations initially coexist from the excitation pulse and then evolve from one into the other. The 471 nm and 565 nm kinetics both exhibit a non-monotonic kinetics. The initial decay has a time constant of 175 fs at 292 K that slows to 700 fs at 140 K (well outside our 125 fs instrumental response). At the far-red region near 645 nm, we can see from both the kinetics and the EADS3 and EADS4 that the 645 nm band decays, while the 565 nm grows in the 2–4 ns time scale.

These data and the EADS analysis are supportive of an inhomogeneous set of populations involved in the photodynamics with evolution from one state to another. Based on the EADS analysis and given the fact that there are multiple closely-spaced charge-transfer transitions in the pump wavelength region of the steady-state absorption spectra of 2Fe-2S ferredoxins,[3–4] efforts were made to analyze and interpret the TA data using a more complex four-state combined inhomogeneous parallel-sequential target model (Figure S6–S7). In this model, the pump laser excites the 2Fe-2S cluster to 3 different excited states simultaneously, with the higher states decaying to their nearest lower states. Details of this model can be found in the Supporting Information.

For the ICVS experiment, the 2Fe-2S cluster in Rc6 was excited at 525 nm. The time-dependent absorption changes were observed over a broad wavelength region from 400 nm to 700 nm. The pump pulse excites the S→Fe ligand-to-metal charge-transfer transitions in the 2Fe-2S cluster[3] of Rc6 and promotes a faction of the molecules to electronic excited states, where coherent vibrational wave-packets are launched.[19] The kinetics of the ICVS data are nearly identical to the TA signals in Figure 2, but overlaid with oscillatory components decaying within a few picoseconds. Unfortunately, the cross-phase-modulation artifact[20] lasts for about 100 fs (Figure S3) and prevents the characterization of <100 fs dynamics and we limited our analysis to time delays longer than 100 fs.

Figure 4 (A) contrasts the ICVS kinetic traces for 525 nm probe wavelength at both 292 K and 140 K with baseline fits. To separate the oscillatory components of these signals from the population dynamics discussed above, the target model proposed in Figure S6 for the TA study was used to fit the ICVS data (black curves in Figure 4(A)) and the fitting curves are subtracted from the raw data to obtain the residuals (Figure S8). A FT analysis was performed on the residuals and the resulting maps of the FT power spectra of the residuals at both 292 K and 140 K are shown in Figure 4 (C) and (D). From the 2D maps, two positive bands at 484 cm^{-1} and 417 cm^{-1} for both 292 K and 140 K are clearly resolved. However, the intensity of the 484 cm^{-1} band increased significantly at 140 K compared to 292 K. At some probe wavelength, the 417 cm^{-1} peak almost disappeared at 292 K. The FT intensity spectra for 525 nm probe wavelength are shown in Figure 4 (B), which shows the same temperature effect as the 2D maps.

The 417 cm^{-1} band in the 140 K ICVS data is consistent with resonance Raman and normal mode calculations for Rc6 at 77 K,[21] as well as for other 2Fe-2S ferredoxins such as putidaredoxin[22] and *Aquifex aeolicus* ferredoxin 5.[21] It was assigned as the $B_{2u}{}^{b}$ asymmetric Fe-S^{b} stretching mode in idealized D_{2h} symmetry for the $Fe_2S^{b}{}_2S^{t}{}_4$ core.[21–22]

The 484 cm^{-1} band has not been reported in the 2Fe-2S ferredoxin resonance Raman spectra, nor in more recent IR difference spectra.[23] It is a higher frequency than most of the Fe-S related normal modes, but it also does not align as a combination band.[24] Instead, a similar band near this frequency has been observed in room temperature ICVS studies of *Pf*Rd[13] and blue Cu proteins.[25–26] In both samples, it was attributed to excited-state vibrations.

To investigate the nature of these modes, a sliding window Fourier transform (SWFT)[13] of the oscillatory components of the signal was performed on the ICVS data (Figure 5). The 484 cm^{-1} band was initially observed at higher frequency, but slowly shifts to lower frequency within ~600 ps at both temperatures. This is consistent with the multiple excited-state populations that evolve from one state into another. It is likely that the wave-packet evolves from the highest excited-electronic-state potential-energy surface to the lower-lying states after excitation. Since the electronic structure of the active site differs at different electronic states, it is reasonable to observe shifting of the vibrational frequency of the excited-state vibrations. Similar phenomena have been reported before.[27] The SWFT also shows that the 417 cm^{-1} band has a slightly longer lifetime and appears slightly later than the 484 cm^{-1} band, suggesting an assignment of the 484 cm^{-1} band to a rapidly-decaying excited state. However, the difference in lifetimes was not significant enough for a decisive conclusion.

The temperature dependence of the relative intensity or existence of the two vibrational bands was surprising to observe. Fraser and co-workers recently reported that cryocooling suppresses or modifies protein conformation heterogeneities.[28] We postulate that temperature change either slightly perturbs the structure/geometry of the active site and its surrounding amino acids of Rc6, or that different temperature favors different conformations of the protein, and thus affects the relative intensity or existence of the vibrational modes observed. This phenomenon suggests that temperature effect to the structure or

conformational heterogeneities of iron-sulfur proteins needs to be carefully considered when interpreting experimental data often collected at cryogenic temperatures (e.g., EPR, cryo-FTIR and Mossbauer spectroscopies).

The TA signals argue that laser excitation of the 2Fe-2S cluster of Rc6 generates multiple excited-state populations, which result in complicated multi-phasic dynamics. This is not surprising since there are multiple charge-transfer transitions proposed from electronic structure calculations in the visible region for 2Fe-2S clusters[3–4] and the bandwidth of the pump laser overlaps with several of them (Figure 6A). As early as 1984, Noodleman and coworkers calculated dozens of electronic transitions for the near IR and visible region alone.[3] According to Noodleman's predictions, the three charge transfer bands that excited by the 525 nm pump (Figure 6A) are 519 nm (opp. S, S* → Fe), 536 nm (opp. S, S* → Fe), and 546 nm (S, S*→ Fe).[3] More recently, Neese and coworkers suggest that the simple double-exchange model underestimates the true density of low-lying states by one to two orders of magnitude, which further complicate the interpretation of photoinduced dynamics in these systems.[4]

The simultaneous excitation of several excited-state populations also indicates that during the ICVS experiment, multiple wave-packets are simultaneously launched on multiple electronic states. This might be a disadvantage if the vibrations on a single excited electronic state of FeS proteins are to be studied. However, it allows us to observe vibrational modes on multiple electronic excited states and provides helpful information for theoretical simulations of excited-state vibrations in FeS clusters. In particular, these modes are not accessible by steady-state vibrational techniques such as Resonance Raman that are primarily sensitive to ground-state vibrations.

The long lifetimes of the lower excited electronic states (2.45 ns for 292 K and 4.49 ns for 140 K) are significantly longer than that of *Pf*Rd[13] and FeMoco[14] in the nitrogenase MoFe protein, suggesting that 2Fe-2S clusters like in Rc6 are potential candidates as external photosensitizers for light-induced hydrogen production in hydrogenase or hydrogenase model compounds.[9] The longer the lifetimes of these charge-transfer populations, the greater the opportunity to take advantage of them for productive redox chemistry like light-induced hydrogen generation. The proximity of the 2Fe-2S cluster to the protein surface (Figure S9) also makes it easier to use 2Fe-2S clusters as photosensitizers.

The TA data together with the EADS and extracted timescales (Table S1) and target analyses suggest that there are clearly two long-lived states that co-exist (Figures 2 and 3). One resembles the 500 ps TA spectrum shown in Figure 6B, whereas the other is a positive band at 645 nm. The 645 nm band decays within 1.5 ns, but the other population persists up to 2.45 ns at 292 K and 4.49 ns at 140 K. Interestingly, the TA spectra at 500 ps for both temperatures strongly resemble the reduced–oxidized steady-state difference spectra (Figure 6B). This suggests that the longer-lived state is probably due to a photo-induced long-range "external" ET transition illustrated by Scheme 1 (ET Path 2). This is in agreement with the electronic structure calculations by Noodleman et al.,[3] where the 525 nm pump laser excites the ET transitions from the opposite cysteine-thiol to an iron (Opp. S → Fe). It is possible that the pump laser induces a transient reduction of the 2Fe-2S cluster by promoting one

electron to move from a cysteine-thiol to the opposite iron while another electron from a nearby amino acid fills the hole on the cysteine. After laser excitation, the electron returns to its original location. This partial reduction persists for a few ns and is consistent with the larger barrier for a long-range ET from an external amino acid to the cysteine-thiol and then to an opposite iron. To further investigate this long-range "external" ET pathway, efforts were made to identify potential hole-transfer (HT) pathways in Rc6 because ET from amino acids requires the quenching of holes. Recently, HT pathways in proteins have been investigated in multiple metalloproteins where linear/branched chains of tryptophan and tyrosine residues serve as potential HT pathways due to their lower redox potentials through changing their protonized states.[29–31] Close examination of the crystal structure of Rc6 reveals that Cys48 is directly bonded with His-49 whose imidazole side-chain is only 4.7 angstroms from the aromatic ring of Tyr51. The later is 7.7 angstroms from Tyr75, and both Tyr51 and Tyr75 are close to the protein surface (Scheme 1). Thus, the electron holes created by the long-range ET can be quenched through the HT pathways: Cys48 → His49 → Tyr51 (and/or → Tyr75) (Scheme 1).The Trp56 residue of Rc6 is more than 16 angstroms from the active site and surrounding amino acids and thus does not participate in the HT pathways. The shorter-lived state (1.23 ns for 292 K and 1.42 ns for 140 K) may be attributed to the transient internal ET from a bridging-sulfide or a neighboring cysteine-thiol to iron (ET Path 1 in Scheme 1). These results suggest a potential light-induced long-range ET pathway might exist in 2Fe-2S ferredoxins. Similar photo-induced ET pathways have been observed in other ET metalloenzymes.[6, 26, 32]

To conclude, the ultrafast electronic and vibrational relaxation dynamics of Rc6 were characterized. The TA signals revealed that multiple ligand-to-metal charge-transfer populations were induced by laser excitation that evolve into low-lying states. Two long-lived states were identified, with the longer one attributed to a long-range "*external*" ET, which suggests the potential existence of a photo-induced long-range ET pathway in FeS proteins. The existence of potential HT pathways consisting of a chain of histidine and tyrosines near Cys48 affirms the existence of this long-range ET pathway. The shorter-lived state is ascribed to a transient *internal* ET from a nearby sulfur to iron. The excited-state population transfer is consistent with the slight shifting the 484 cm^{-1} ICVS band first observed in Rc6 and attributed to excited-electronic-state vibrations. Exactly how this band may contribute to ET and redox properties of FeS clusters is a topic of further study (manuscript in preparation). The temperature effect to the ICVS spectra suggests that temperature effect deserves consideration during the study of FeS proteins at cryogenic temperatures. The study on 2Fe-2S ferredoxins' ultrafast electronic and vibrational dynamics lays a foundation for future characterization of larger FeS clusters in proteins.

Supplementary Material

Refer to Web version on PubMed Central for supplementary material.

ACKNOWLEDGMENT

We thank Jacques Meyer from CEA-Grenoble at France for generously providing the Rc6 sample. This work was funded by NSF CHE-1413739 (D.S.L.), NSF CHE-0745353 (S.P.C.) and NIH GM65440 (S.P.C.).

REFERENCES

1. Lill R Function and biogenesis of iron-sulphur proteins. Nature 2009, 460 (7257), 831–838. [PubMed: 19675643]
2. Johnson DC; Dean DR; Smith AD; Johnson MK Structure, function, and formation of biological iron-sulfur clusters. Annu. Rev. Biochem 2005, 74, 247–281. [PubMed: 15952888]
3. Noodleman L; Baerends EJ Electronic-Structure, Magnetic-Properties, Electron-Spin-Resonance, and Optical-Spectra for 2-Fe Ferredoxin Models by Lcao-X-Alpha Valence Bond Theory. J. Am. Chem. Soc 1984, 106 (8), 2316–2327.
4. Sharma S; Sivalingam K; Neese F; Chan GKL Low-energy spectrum of iron-sulfur clusters directly from many-particle quantum mechanics. Nat. Chem 2014, 6 (10), 927–933. [PubMed: 25242489]
5. Kim CS; Jung J Iron Sulfur Centers as Endogenous Blue-Light Sensitizers in Cells - a Study with an Artificial Nonheme Iron Protein. Photochem. Photobiol 1992, 56 (1), 63–68. [PubMed: 1508984]
6. Hochkoeppler A; Zannoni D; Ciurli S; Meyer TE; Cusanovich MA; Tollin G Kinetics of photo-induced electron transfer from high-potential iron-sulfur protein to the photosynthetic reaction center of the purple phototroph Rhodoferax fermentans. Proc. Natl. Acad. Sci. U.S.A 1996, 93 (14), 6998–7002. [PubMed: 8692932]
7. Brown KA; Dayal S; Ai X; Rumbles G; King PW Controlled Assembly of Hydrogenase-CdTe Nanocrystal Hybrids for Solar Hydrogen Production. J. Am. Chem. Soc 2010, 132 (28), 9672–9680. [PubMed: 20583755]
8. Brown KA; Harris DF; Wilker MB; Rasmussen A; Khadka N; Hamby H; Keable S; Dukovic G; Peters JW; Seefeldt LC; King PW Light-driven dinitrogen reduction catalyzed by a CdS:nitrogenase MoFe protein biohybrid. Science 2016, 352 (6284), 448–450. [PubMed: 27102481]
9. Adam D; Bosche L; Castaneda-Losada L; Winkler M; Apfel P; Happe T Sunlight-Dependent Hydrogen Production by Photosensitizer/Hydrogenase Systems. Chemsuschem 2017, 10 (5), 894–902. [PubMed: 27976835]
10. Wang WG; Rauchfuss TB; Bertini L; Zampella G Unsensitized Photochemical Hydrogen Production Catalyzed by Diiron Hydrides. J. Am. Chem. Soc 2012, 134 (10), 4525–4528. [PubMed: 22364563]
11. Armengaud J; Meyer C; Jouanneau YA [2Fe-2S] ferredoxin (FdVI) is essential for growth of the photosynthetic bacterium Rhodobacter capsulatus. J. Bacteriol 1997, 179 (10), 3304–3309. [PubMed: 9150228]
12. Sainz G; Jakoncic J; Sieker LC; Stojanoff V; Sanishvili N; Asso M; Bertrand P; Armengaud J; Jouanneau Y Structure of a [2Fe-2S] ferredoxin from Rhodobacter capsulatus likely involved in Fe-S cluster biogenesis and conformational changes observed upon reduction. J. Biol. Inorg. Chem 2006, 11 (2), 235–246. [PubMed: 16402206]
13. Tan ML; Bizzarri AR; Xiao YM; Cannistraro S; Ichiye T; Manzoni C; Cerullo G; Adams MWW; Jenney FE; Cramer SP Observation of terahertz vibrations in Pyrococcus furiosus rubredoxin via impulsive coherent vibrational spectroscopy and nuclear resonance vibrational spectroscopy - interpretation by molecular mechanics. J. Inorg. Biochem 2007, 101 (3), 375–384. [PubMed: 17204331]
14. Delfino I; Cerullo G; Cannistraro S; Manzoni C; Polli D; Dapper C; Newton WE; Guo YS; Cramer SP Observation of Terahertz Vibrations in the Nitrogenase FeMo Cofactor by Femtosecond Pump-Probe Spectroscopy. Angew. Chem. Int. Ed 2010, 49 (23), 3912–3915.
15. Maiuri M; Delfino I; Cerullo G; Manzoni C; Pelmenschikov V; Guo YS; Wang HX; Gee LB; Dapper CH; Newton WE; Cramer SP Low frequency dynamics of the nitrogenase MoFe protein via femtosecond pump probe spectroscopy - Observation of a candidate promoting vibration. J. Inorg. Biochem 2015, 153, 128–135. [PubMed: 26343576]
16. van Stokkum IHM; Larsen DS; van Grondelle R Global and target analysis of time-resolved spectra. Biochim. Biophys. Acta, Bioenerg 2004, 1657 (2–3), 82–104.
17. Holzwarth AR Data Analysis of Time-Resolved Measurements In Biophysical techniques in photosynthesis; Amesz J; Hoff AJ, Eds. Springer: Dordrecht, The Netherlands, 1996; pp 75–92.
18. Larson EJ; Johnson CK Temperature-dependent study of the ultrafast photophysics of all-trans retinal. J. Phys. Chem. B 1999, 103 (49), 10917–10923.

19. Fragnito HL; Bigot JY; Becker PC; Shank CV Evolution of the Vibronic Absorption-Spectrum in a Molecule Following Impulsive Excitation with a 6 Fs Optical Pulse. Chem. Phys. Lett 1989, 160 (2), 101–104.
20. Kovalenko SA; Dobryakov AL; Ruthmann J; Ernsting NP Femtosecond spectroscopy of condensed phases with chirped supercontinuum probing. Phys. Rev. A 1999, 59 (3), 2369–2384.
21. Xiao YM; Tan ML; Ichiye T; Wang HX; Guo YS; Smith MC; Meyer J; Sturhahn W; Alp EE; Zhao JY; Yoda Y; Cramer SP Dynamics of Rhodobacter capsulatus [2Fe-2S] ferredoxin VI and Aquifex aeolicus ferredoxin 5 via nuclear resonance vibrational spectroscopy (NRVS) and resonance Raman spectroscopy. Biochemistry 2008, 47 (25), 6612–6627. [PubMed: 18512953]
22. Fu WG; Drozdzewski PM; Davies MD; Sligar SG; Johnson MK Resonance Raman and Magnetic Circular-Dichroism Studies of Reduced [2fe-2s] Proteins. J. Biol. Chem 1992, 267 (22), 15502–15510. [PubMed: 1639790]
23. Khalil M; Bernhardt R; Hellwig P Raman and infrared spectroscopic evidence for the structural changes of the 2Fe-2S cluster and its environment during the interaction of adrenodoxin and adrenodoxin reductase. Spectrochim. Acta, Part A 2017, 183, 298–305.
24. Han S; Czernuszewicz RS; Kimura T; Adams MWW; Spiro TG Fe2s2 Protein Resonance Raman-Spectra Revisited - Structural Variations among Adrenodoxin, Ferredoxin, and Red Paramagnetic Protein. J. Am. Chem. Soc 1989, 111 (10), 3505–3511.
25. Cimei T; Bizzarri AR; Cerullo G; De Silvestri S; Cannistraro S Excited state charge-transfer dynamics study of poplar plastocyanin by ultrafast pump-probe spectroscopy and molecular dynamics simulation. Biophys. Chem 2003, 106 (3), 221–231. [PubMed: 14556894]
26. Book LD; Arnett DC; Hu HB; Scherer NF Ultrafast pump-probe studies of excited-state charge-transfer dynamics in blue copper proteins. J. Phys. Chem. A 1998, 102 (23), 4350–4359.
27. Kobayashi T; Saito T; Ohtani H Real-time spectroscopy of transition states in bacteriorhodopsin during retinal isomerization. Nature 2001, 414 (6863), 531–534. [PubMed: 11734850]
28. Keedy DA; van den Bedem H; Sivak DA; Petsko GA; Ringe D; Wilson MA; Fraser JS Crystal Cryocooling Distorts Conformational Heterogeneity in a Model Michaelis Complex of DHFR. Structure 2014, 22 (6), 899–910. [PubMed: 24882744]
29. Gray HB; Winkler JR Hole hopping through tyrosine/tryptophan chains protects proteins from oxidative damage. Proc. Natl. Acad. Sci. U.S.A 2015, 112 (35), 10920–10925. [PubMed: 26195784]
30. Winkler JR; Gray HB Electron flow through biological molecules: does hole hopping protect proteins from oxidative damage? Q. Rev. Biophys 2015, 48 (4), 411–420. [PubMed: 26537399]
31. Sun WC; Dai HJ; Tao Y; Xiao D; Zhang YF; Wei ZD; Chen XH Potent Relay Stations for Electron Transfer in Proteins: pi therefore pi Three-Electron Bonds. J. Phys. Chem. C 2013, 117 (36), 18325–18333.
32. Edington MD; Diffey WM; Doria WJ; Riter RE; Beck WF Radiationless decay from the ligand-to-metal charge-transfer state in the blue copper protein plastocyanin. Chem. Phys. Lett 1997, 275 (1–2), 119–126.

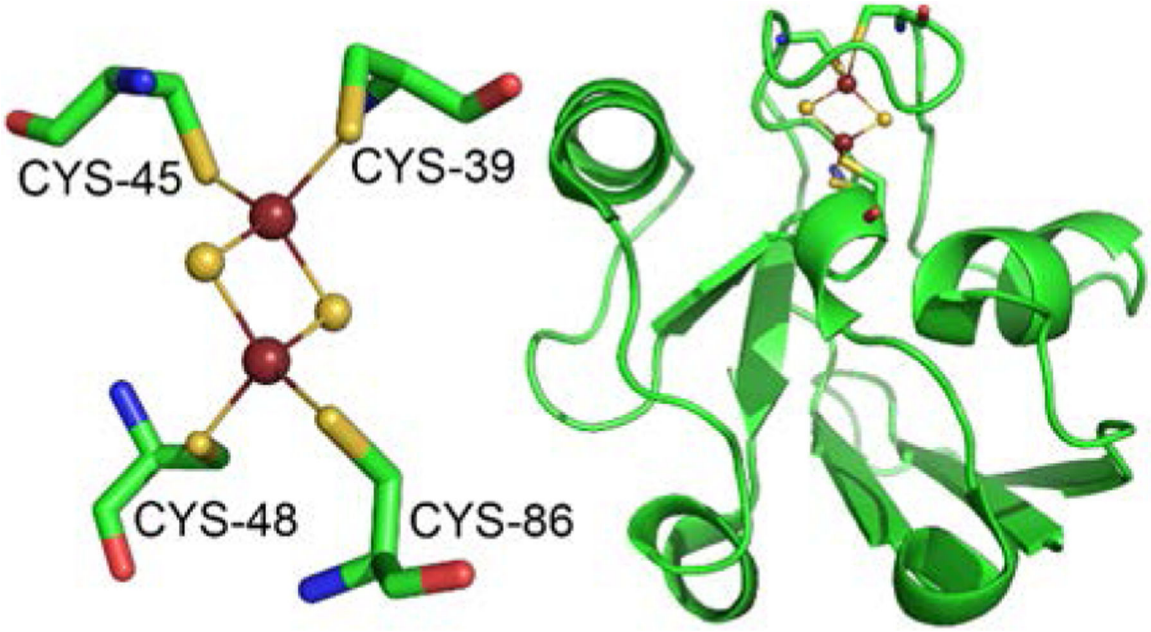

Figure 1:
Oxidized Rc6 active site structure. (Left) 2Fe-2S cluster structure and (Right) full protein structure (PDB: 1E9M). Colors for atoms: Fe (brick), S (yellow), C (green), N (blue), O (red).

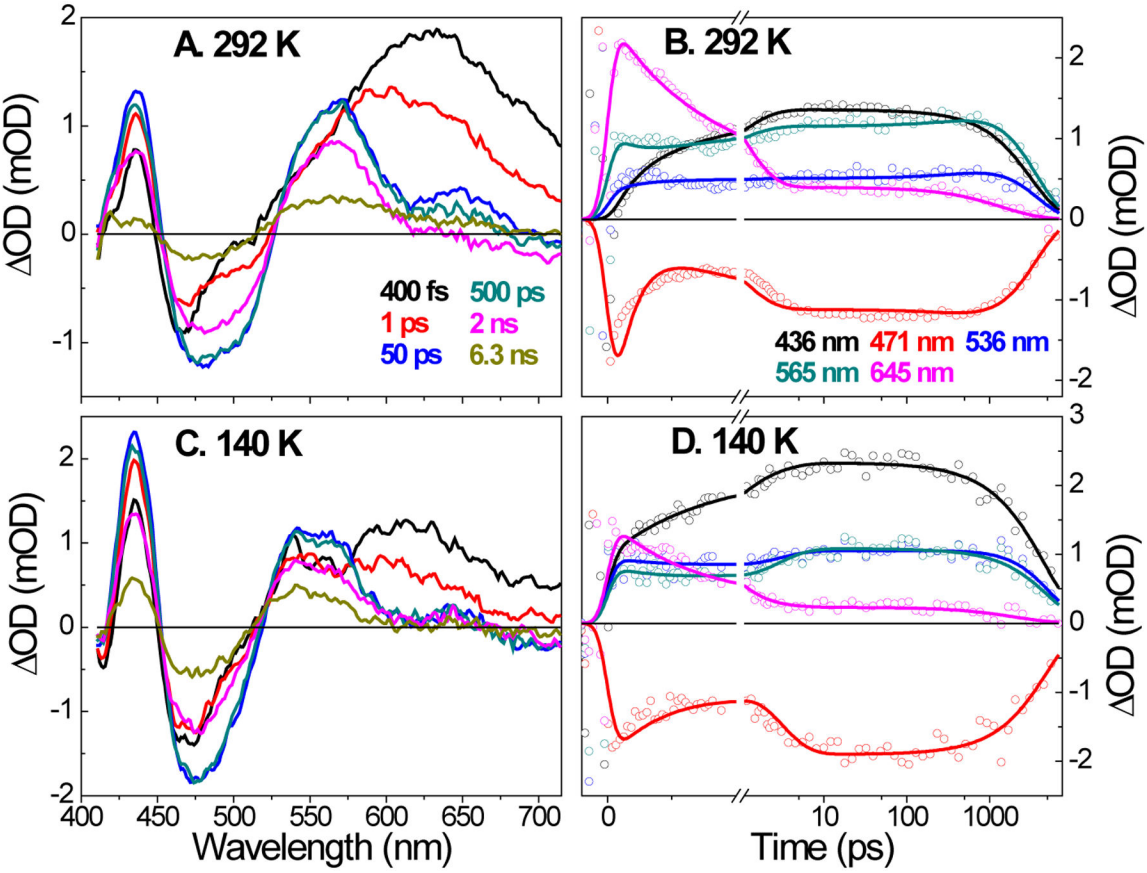

Figure 2:

Transient spectra at select probe time (A for 292 K and C for 140 K) and kinetics at select wavelengths (B for 292 K and D for 140 K). For panels B and D, the open circles are for the raw data and the solid curves are fits to the raw data using the sequential model in Figure 3.

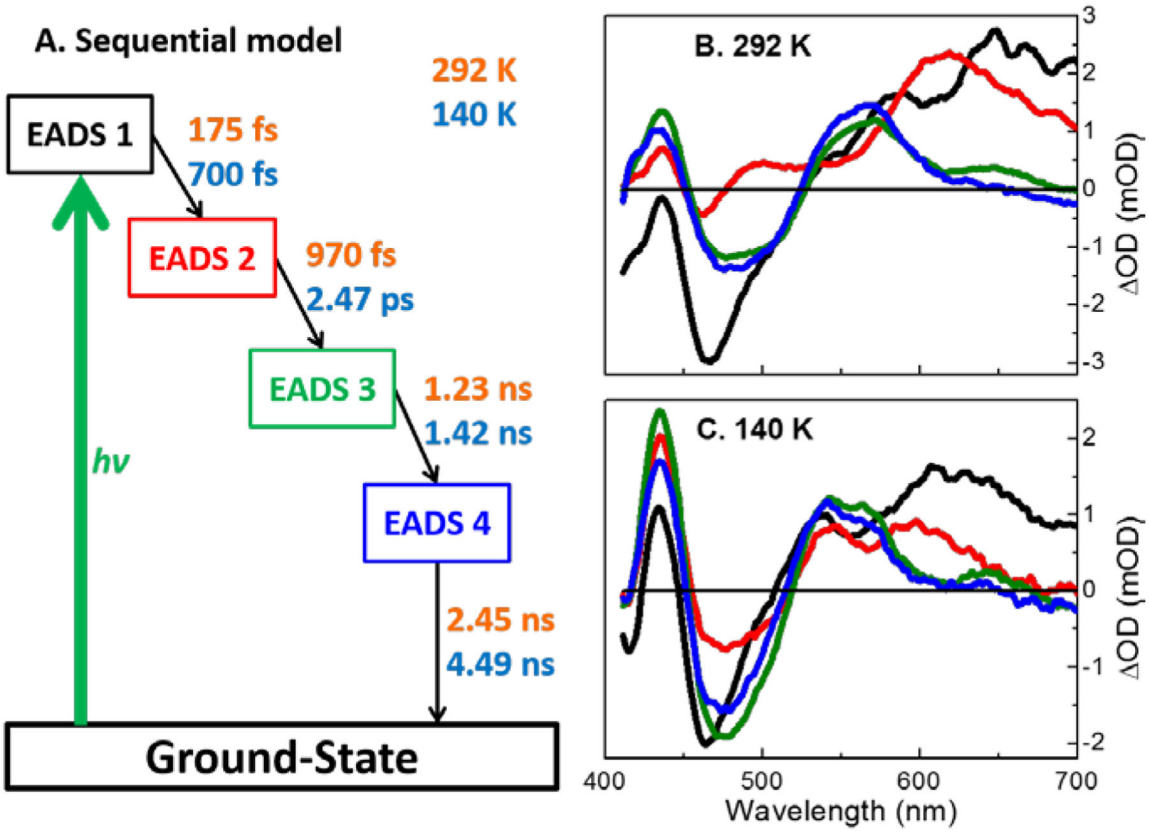

Figure 3:

(A) Four-compartment sequential model to describe the data. Time constants for 292 K are in orange and 140 K are in cyan. (B and C) Extracted EADS for the fit of the sequential model to the 292 K (B) and 140 K (C) data. The evolution profiles for these EADS are contrasted in Figure S4. The colors of the EADS are the same as those in panel (A): EADS1 (black), EADS2 (red), EADS3 (olive), EADS4 (blue).

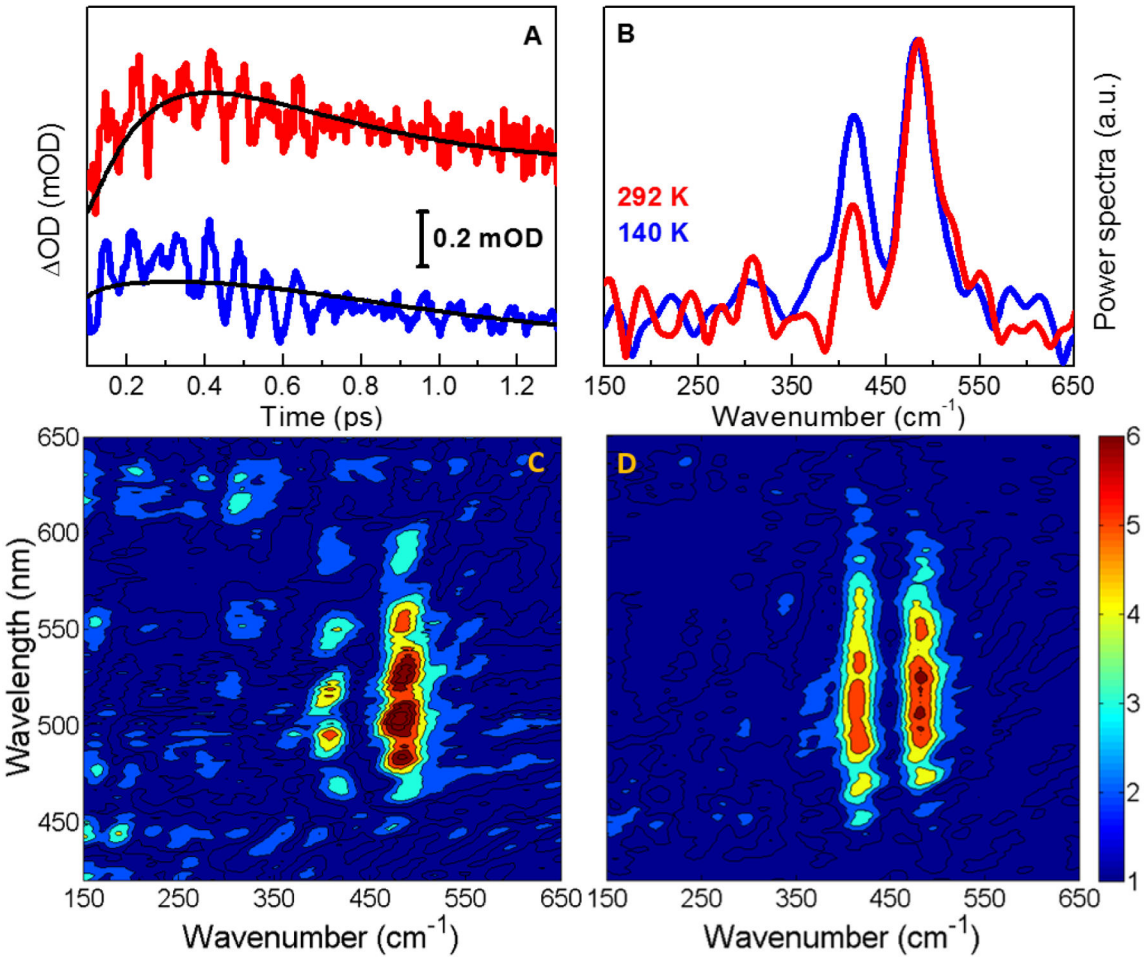

Figure 4:

(A) Oscillatory components and fits using the target model proposed in Figure S6 for 525 nm probe wavelength at 292 K (red) and 140 K (blue). (B) Power spectra obtained for 525 nm probe wavelength at 292 K (red) and 140 K (blue). (C) 2D power spectra at 292 K. (D) 2D power spectra at 140 K. Only the kinetics within the first 2 ps following laser excitation were collected for the investigation of the vibrational relaxation dynamics of Rc6.

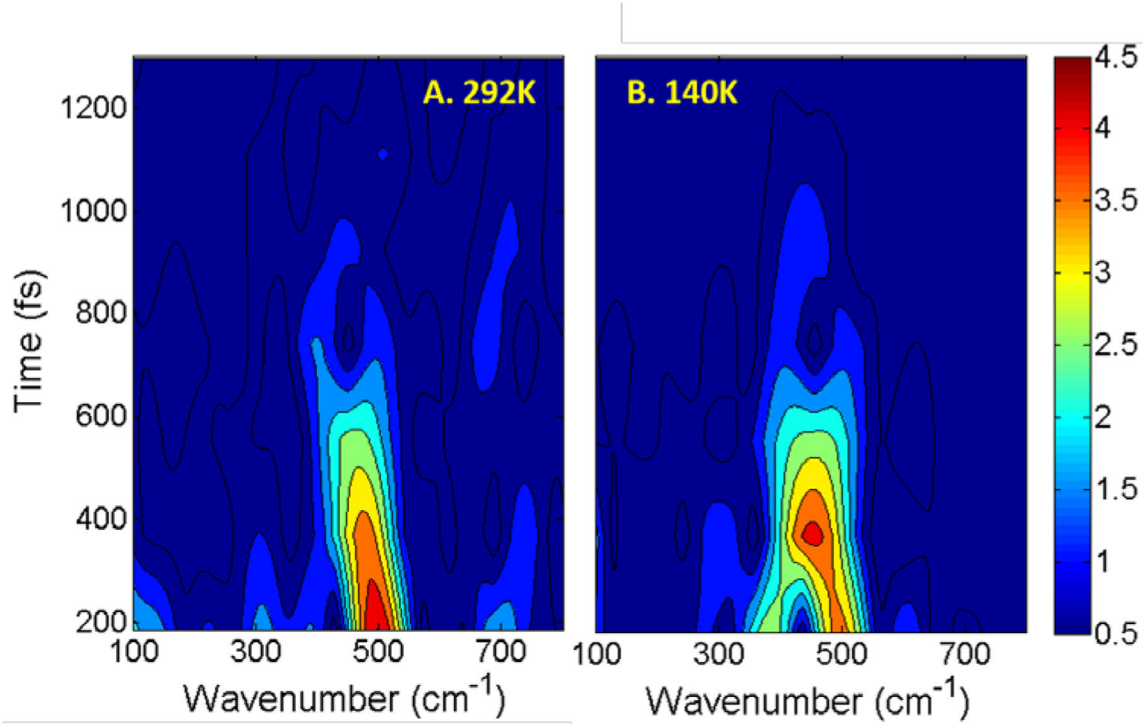

Figure 5.

Spectrogram obtained by performing the sliding window Fourier transform of the oscillatory component of the signal at 525 nm probe wavelength at (A) 292 K and (B) 140 K. The calculations used 6th order super Gaussian function and 370 fs window.

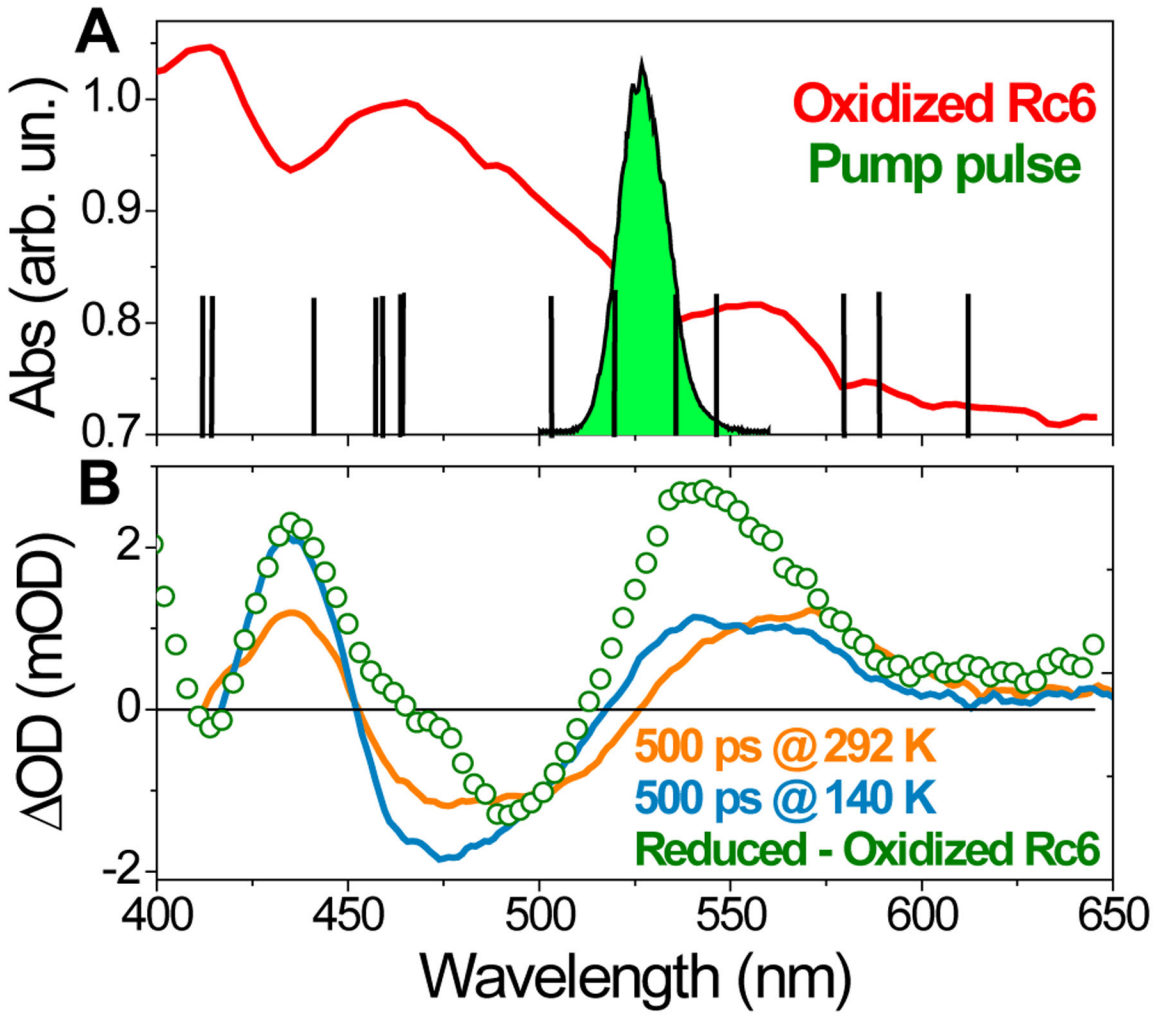

Figure 6:

(A) Static absorption spectrum for oxidized Rc6 (red) overlaid with pump laser spectrum (green). The vertical black bars are the charge transfer bands predicted by Noodleman et al., [3] the blue curved arrows indicate excited state population transfers following laser excitation. (B) Transient absorption spectra at 500 ps for 292 K (orange) and 140 K (cyan) overlaid with the static difference absorption spectrum (olive, open circles) obtained by subtracting the absorption spectrum of oxidized Rc6 from that of reduced Rc6. Static absorption spectra data taken from (Sainz et al., 2006)[12]

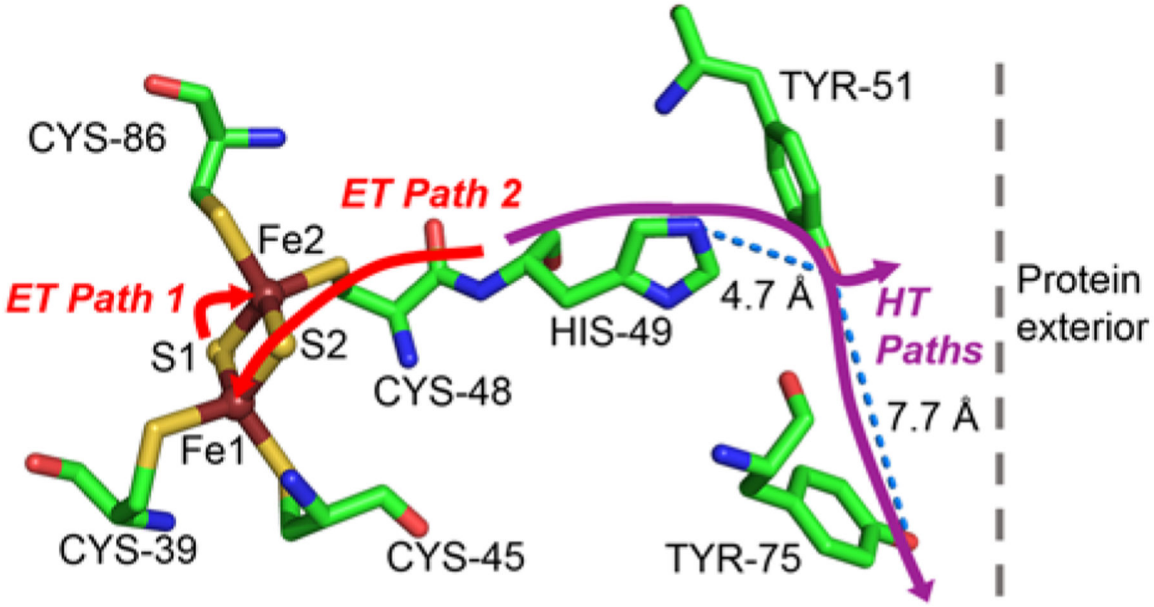

Scheme 1.

Proposed electron-transfer and hole-transfer pathways. Color coding: Electron-transfer (ET) pathways are denoted with red arrowed lines and hole-transfer (HT) pathways with purple arrowed lines.